Search for Extreme Mass Ratio Inspirals with LISA.

Stanislav Babak

Max Planck Institute for Gravitational Physics
(Albert Einstein Institute)
Potsdam-Golm, Germany

19-23 June, 2017, Rome

Overview

Gravitational waves landscape

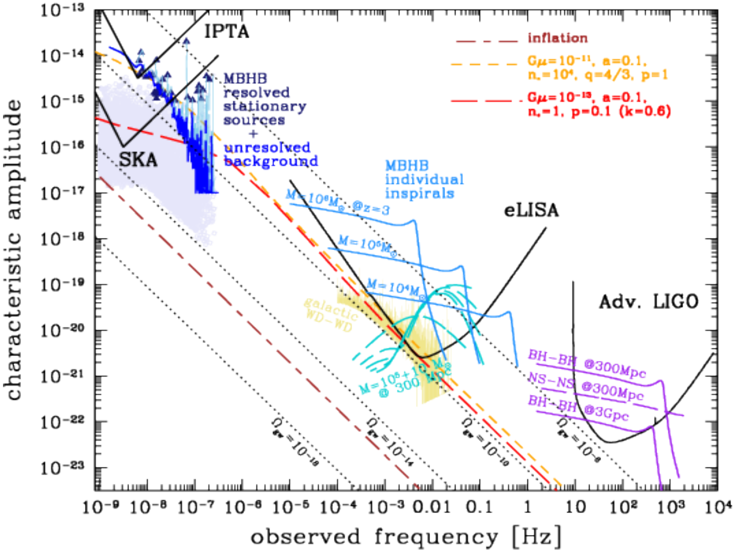

[credits: A. Sesana]

Detection of GW with LIGO

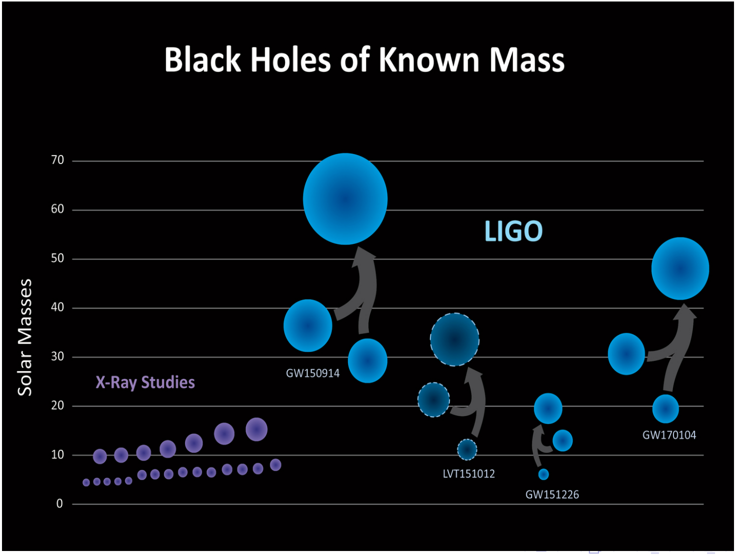

Detection of GW with LIGO

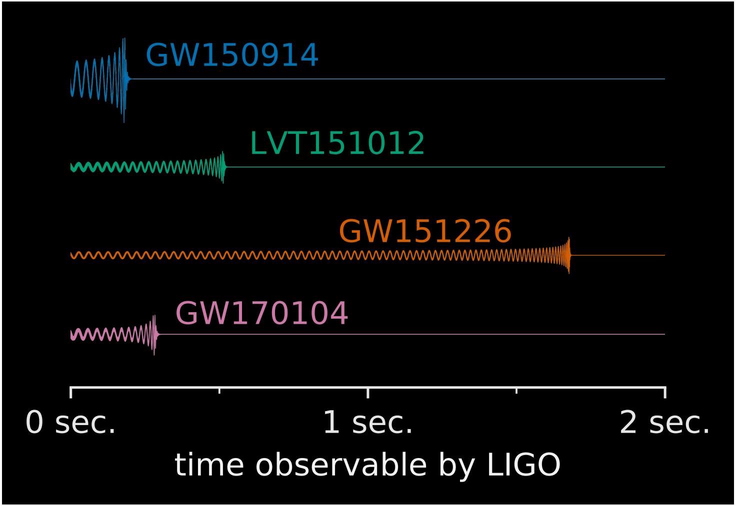

LISA: laser interferometer in space.

- LISA is a future space based GW observatory, to be launched around 2034.
- LISA Pathfinder: very successful demonstration of LISA technologies.

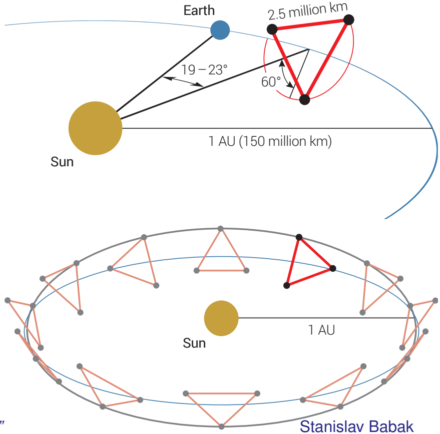

LISA: laser interferometer in space.

- LISA is a future space based GW observatory, to be launched around 2034.
- LISA Pathfinder: very successful demonstration of LISA technologies.

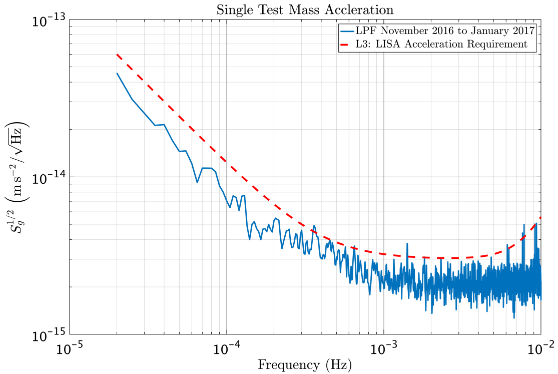

LISA data analysis challenges

- LISA data will be signal dominated. Signals are strong and long lived
- LISA data will contain simultaneously thousands of signals, which we need to individually resolve and characterize
- LISA data will contain non-stationary noise

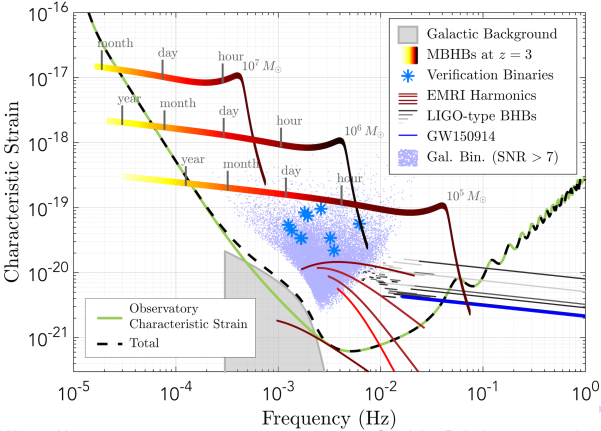

Extreme mass ratio inspirals (EMRIs)

- EMRI: capture of a small compact object (CO) (white dwarf, neutron star or stellar mass black hole) by a massive black hole (MBH) in the centre of a galaxy.
- extreme mass ratio: $m/M \sim 10^{-7} - 10^{-4}$ - small parameter
- Inspiral: CO spends $10^4 - 10^6$ orbits in close vicinity of a MBH before it plunges

Let us cook up an EMRI: ingredients

- we need MBH
- we need CO in close vicinity
- we need to form a GW-driven binary MBH-CO
- EMRI should be detectable (high enough signal-to-noise ratio (SNR))
- we should have all necessary tools to detect EMRI

Extreme mass ratio inspirals (EMRIs)

- EMRI: capture of a small compact object (CO) (white dwarf, neutron star or stellar mass black hole) by a massive black hole (MBH) in the centre of a galaxy.
- extreme mass ratio: $m/M \sim 10^{-7} - 10^{-4}$ - small parameter
- Inspiral: CO spends $10^4 - 10^6$ orbits in close vicinity of a MBH before it plunges

Let us cook up an EMRI: ingredients

- we need MBH
- we need CO in close vicinity
- we need to form a GW-driven binary MBH-CO
- EMRI should be detectable (high enough signal-to-noise ratio (SNR))
- we should have all necessary tools to detect EMRI

Extreme mass ratio inspirals (EMRIs)

- EMRI: capture of a small compact object (CO) (white dwarf, neutron star or stellar mass black hole) by a massive black hole (MBH) in the centre of a galaxy.
- extreme mass ratio: $m/M \sim 10^{-7} - 10^{-4}$ - small parameter
- Inspiral: CO spends $10^4 - 10^6$ orbits in close vicinity of a MBH before it plunges

Let us cook up an EMRI: ingredients

- we need MBH
- we need CO in close vicinity
- we need to form a GW-driven binary MBH-CO
- EMRI should be detectable (high enough signal-to-noise ratio (SNR))
- we should have all necessary tools to detect EMRI

Extreme mass ratio inspirals (EMRIs)

- EMRI: capture of a small compact object (CO) (white dwarf, neutron star or stellar mass black hole) by a massive black hole (MBH) in the centre of a galaxy.
- extreme mass ratio: $m/M \sim 10^{-7} - 10^{-4}$ - small parameter
- Inspiral: CO spends $10^4 - 10^6$ orbits in close vicinity of a MBH before it plunges

Let us cook up an EMRI: ingredients

- we need MBH
- we need CO in close vicinity
- we need to form a GW-driven binary MBH-CO
- EMRI should be detectable (high enough signal-to-noise ratio (SNR))
- we should have all necessary tools to detect EMRI

Extreme mass ratio inspirals (EMRIs)

- EMRI: capture of a small compact object (CO) (white dwarf, neutron star or stellar mass black hole) by a massive black hole (MBH) in the centre of a galaxy.
- extreme mass ratio: $m/M \sim 10^{-7} - 10^{-4}$ - small parameter
- Inspiral: CO spends $10^4 - 10^6$ orbits in close vicinity of a MBH before it plunges

Let us cook up an EMRI: ingredients

- we need MBH
- we need CO in close vicinity
- we need to form a GW-driven binary MBH-CO
- EMRI should be detectable (high enough signal-to-noise ratio (SNR))
- we should have all necessary tools to detect EMRI

Massive BHs

- We expect that all galaxies host MBH in their nuclei.
- Milky Way Galaxy: bright O-B stars orbiting dark massive $M \approx 4 \times 10^6 M_\odot$ compact object $\rightarrow$ massive black hole (MBH).

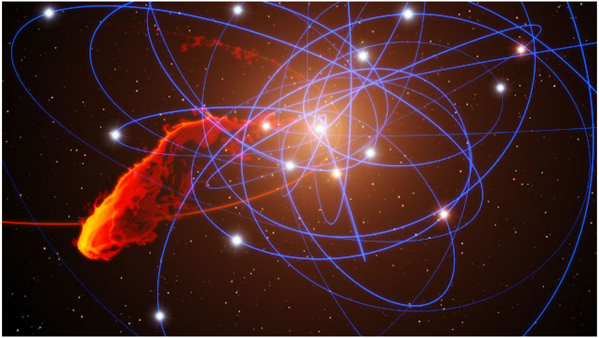

MBH parameters

- Only BHs in the range $M \in [10^4, 10^7] M_\odot$ accessible to LISA
- We do not have direct measure of MBH mass: selection effect, $M - \sigma$ relation
- Model of the MBH evolution from initial seeds to MBH observed now (accretion, galactic mergers)

$$\frac{dn}{d \log M} = A \left(\frac{M}{3 \times 10^6 M_\odot} \right)^\beta \mathrm{Mpc}^{-3},$$

  where $A \simeq 0.002 - 0.005$ and $\beta \simeq -0.3 - 0.3$. [Barausse+ 2012, Sesana+ 2014, Antonini+ 2015]
- Accretion is the main mechanism $\rightarrow$ spin up of MBHs $\rightarrow$ spin could be $a > 0.9$

Stellar cusp

- Mass segregation: stars interact gravitationally $\rightarrow$ divide the kinetic energy equally $\rightarrow$ more massive objects to sink deeper in the potential well of the MBH.
- Stellar mass BHs form a "cusp" (power-law density) $n(r) \sim r^{-\alpha}$, $\alpha \simeq 1.7 - 2$ [Alexander & Hopman 2009]

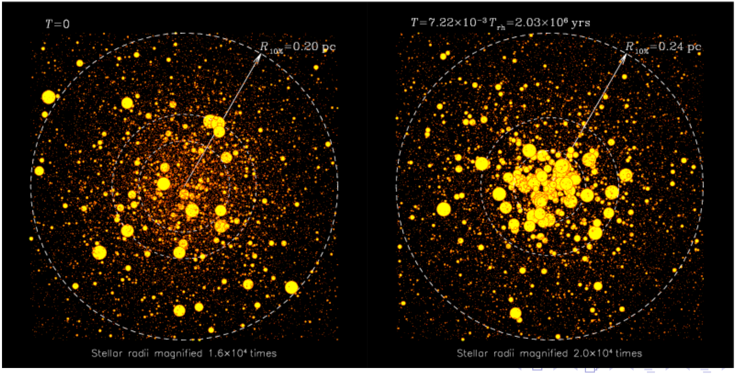

EMRI formation

- 2-body relaxation: mutual gravitational deflection and contact collisions of COs in the cusp. Result is either direct plunge or slow inspiral (bursts of GW at each periapse passage)
- tidal disruption of binary systems: lightest star is ejected, heavy star is bound

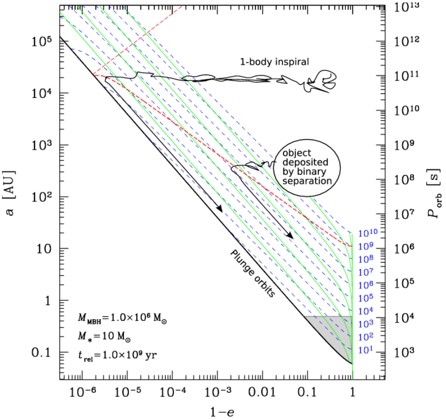

$$R_0 = 300 \left(\frac{M}{10^6 M_\odot} \right)^{-0.19} \mathrm{Gyr}^{-1}.$$ [Amaro-Seoane, Preto 2011]

Event rate computation

- Galaxies merge: leads to erosion of the cusp

Event rate computation

- Galaxies merge: leads to erosion of the cusp
- Some CO plunge directly (instead of steady inspiral)

Event rate computation

- Galaxies merge: leads to erosion of the cusp
- Some CO plunge directly (instead of steady inspiral)
- CO feeding is "not stationary" process (especially for low mass MBH)

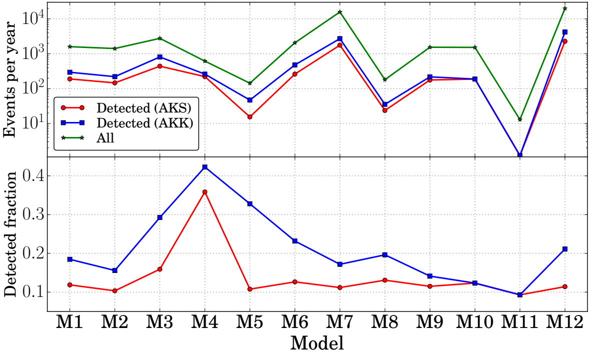

[Babak+ 2017]

Detecting EMRIs

- To detect and estimate parameters we want to use matched filtering
- We need reliable waveforms: need to accurately describe $10^5 - 10^6$ cycles
- We need a data analysis algorithm which could detect this GW signal

Detecting EMRIs

- To detect and estimate parameters we want to use matched filtering
- We need reliable waveforms: need to accurately describe $10^5 - 10^6$ cycles
- We need a data analysis algorithm which could detect this GW signal

Detecting EMRIs

- To detect and estimate parameters we want to use matched filtering
- We need reliable waveforms: need to accurately describe $10^5 - 10^6$ cycles
- We need a data analysis algorithm which could detect this GW signal

Perturbation theory

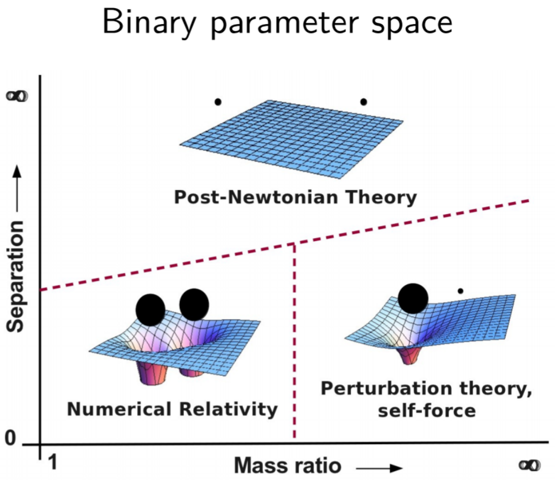

[Leor Barack]

Perturbation theory

- Small mass ratio: $m/M \ll 1$ - small parameter, CO creates small perturbation in the spacetime of MBH.
- The GW signal from EMRIs is rich in structure: three-periodic motion with slowly evolving frequencies

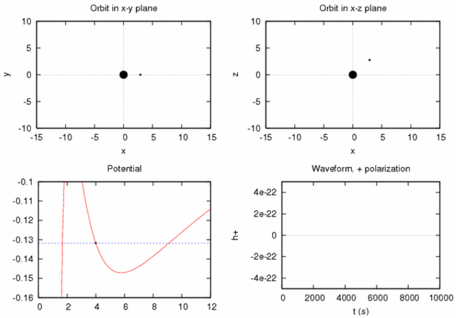

Self-force calculation

- CO can be seen as a small perturber of a Kerr spacetime of MBH
- Near the CO - surrounding is dominated by the self-field, which is "deformed" due to embedding in the field of MBH: not symmetric $\rightarrow$ creates "self-force".
- Near CO gravitational field (spacetime) is matched to the far (w.r.t. CO) field (slightly perturbed Kerr spacetime) $\rightarrow$ equation of motion
- CO can be treated as a point mass: divergence at the position of CO $\rightarrow$ requires regularization (pure mathematical difficulty)
- Self-force: conservative part (time-symmetric, small) + dissipative part (inspiral, dominant)

Self-force calculation

- we want to represent motion as worldline in background
- we want to encode all relevant information about object in multipole moments on worldline

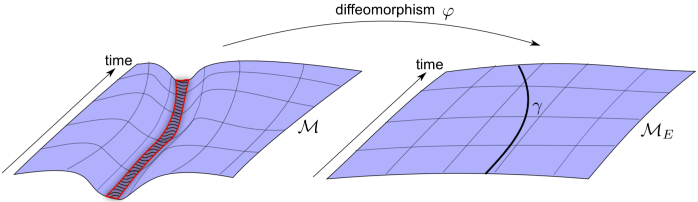

Body in exact spacetime

Representation of motion in external spacetime

[credits A. Pound]

Inspiral using self-force

- Computation of the self-force is expensive!
- Orbital evolution: (i) using only dissipative self-force, (ii) osculating elements approach (iii) self-consistent evolution.
- Progress: generic orbit in Kerr (first order) is under way [M. van de Meent (privat communication)]

Inspiral using self-force

		Schwarzschild circ	Schwarzschild ecc	Kerr circ	Kerr ecc	Kerr incl
Geodesics (analytic)		[Hackmann & Lammerzahl, 2008]		[Fujita & Hikida, 2009] [Hackmann et al, 2010]		
Adiabatic	orbit	[Cutler et al, 1994]		[Shibata et al, 1994]		[Hughes, 1999]
				[Drasco & Hughes, 2006]		
	evolution				[Glamp. & Ken., 2002]	[Hughes, 2001]
				to do		
$\frac{1}{2}$PA: resonances				[Flanagan & Hinderer, 2012] [Flanagan, Hughes & Ruangsri, 2014] [MvdM, 2014]		
1PA:	1GSF	[Barack & Sago, 2007]	[Barack & Sago, 2010]	[Shah et al, 2012]	[MvdM & Shah,2015] [MvdM, 2016]	in progress
	2GSF	in progress	to do	to do		
	spin force	[Papapetrou, 1951]		[Papapetrou, 1951]		
	evolution	[Warburton et al, 2012] [Osburn et al, 2015]		to do		

[credit M.van de Meent]

Approximate models

- We can cheat a bit: we loose accuracy but gain a lot of computational speed $\rightarrow$ develop data analysis methods, assess LISA' scientific capabilities
- *Analytic Kludge* [Barack & Cutler, 2004]: stitching together PN expressions to mimic the underlying physics (periapse and spin-orbital precession). Very fast to generate but not faithful
- *Numerical Kludge* [Babak+ 2007]: use of osculating approach to geodesic (fairly accurate inspiral) & very approximate waveform generation (flat space-time). Slower but more accurate.

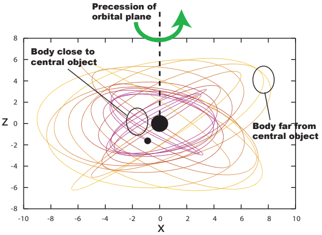

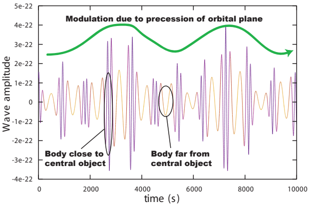

Data analysis challenge

- Geodesic motion in Kerr spacetime can be presented as three-periodic motion [Schmidt 2002, Drasco & Hughes 2003].
- Three corresponding frequencies are slowly evolving (inspiral) under radiation reaction
- This three-periodicity propagates into the EMRI waveform and we see the waveform as harmonics of orbital frequencies

$$h \sim \sum_{kmn} A_{kmn}(t) e^{i(k\phi_r(t) + m\phi_\theta(t) + n\phi_\phi(t))}$$

- Amplitude and phases are functions of intrinsic parameters $m/M, M, \iota(t), p(t), e(t), a$ and initial position. The accurate time evolution should come from the perturbation theory.

Model-dependent solution

- Program "Mock LISA Data Challenge" first started in 2006, then it was suspended in 2011, and resumed 2017 (contact me for more info)
- The simulated data was issued to scientific community, the results to be returned by a deadline
- The last completed challenge contained EMRI signal (based on AK waveform)

MLDC3: EMRis

Source ($\mathrm{SNR_{true}}$)	Group	SNR	$\frac{\delta M}{M}$ $\times 10^{-3}$	$\frac{\delta \mu}{\mu}$ $\times 10^{-3}$	$\frac{\delta \nu_0}{\nu_0}$ $\times 10^{-5}$	δe_0 $\times 10^{-3}$	$\delta \lvert S \rvert$ $\times 10^{-3}$	$\frac{\delta \lambda_{SL}}{\lambda_{SL}}$ $\times 10^{-3}$	δspin (deg)	δsky (deg)	$\frac{\delta D}{D}$
EMRI-1	MTAPCIOA	21.794	5.05	3.29	1.61	-5.1	-1.4	-19	23	2.0	0.07
(21.673)	MTAPCIOA	21.804	-0.06	-0.01	-0.08	-0.05	0.02	0.54	3.5	1.0	0.13
EMRI-2	MTAPCIOA	32.387	-3.64	-2.61	-3.09	3.8	0.87	12	11	3.7	3×10^{-3}
(32.935)	BabakGair	22.790	33.1	-19.7	10.1	-33	-7.3	25	47	3.5	-0.25
	BabakGair	22.850	32.7	-20.0	9.94	-32	-7.2	25	58	3.5	-0.24
	BabakGair	22.801	33.5	-19.5	10.5	-33	-7.4	240	40	3.5	-0.25
EMRI-3	MTAPCIOA	19.598	1.62	0.38	-0.10	-0.35	-0.94	-3.0	5.0	3.0	-0.04
(19.507)	BabakGair	21.392	1.77	1.01	1.95	-1.2	-0.68	-2.3	116	4.5	0.13
	BabakGair	21.364	2.26	1.88	2.71	-2.0	-0.69	-2.5	65	6.1	0.14
	BabakGair	21.362	1.51	1.01	2.09	-1.3	-0.50	-1.7	7.6	6.2	0.14
	EtfAG	—	54.0	4.88	-7375	26	17	—	—	32	0.83

[Babak+ 2010]

MLDC3: EMRIs

Source ($\mathrm{SNR_{true}}$)	Group	SNR	$\frac{\delta M}{M}$ $\times10^{-3}$	$\frac{\delta\mu}{\mu}$ $\times10^{-3}$	$\frac{\delta\nu_0}{\nu_0}$ $\times10^{-5}$	δe_0 $\times10^{-3}$	$\delta\lvert S\rvert$ $\times10^{-3}$	$\frac{\delta\lambda_{SL}}{\lambda_{SL}}$ $\times10^{-3}$	δspin (deg)	δsky (deg)	$\frac{\delta D}{D}$
EMRI-1	MTAPCIOA	21.794	5.05	3.29	1.61	−5.1	−1.4	−19	23	2.0	0.07
(21.673)	MTAPCIOA	21.804	−0.06	−0.01	−0.08	−0.05	0.02	0.54	3.5	1.0	0.13
EMRI-2	MTAPCIOA	32.387	−3.64	−2.61	−3.09	3.8	0.87	12	11	3.7	3×10^{-3}
(32.935)	BabakGair	22.790	33.1	−19.7	10.1	−33	−7.3	25	47	3.5	−0.25
	BabakGair	22.850	32.7	−20.0	9.94	−32	−7.2	25	58	3.5	−0.24
	BabakGair	22.801	33.5	−19.5	10.5	−33	−7.4	240	40	3.5	−0.25
EMRI-3	MTAPCIOA	19.598	1.62	0.38	−0.10	−0.35	−0.94	−3.0	5.0	3.0	−0.04
(19.507)	BabakGair	21.392	1.77	1.01	1.95	−1.2	−0.68	−2.3	116	4.5	0.13
	BabakGair	21.364	2.26	1.88	2.71	−2.0	−0.69	−2.5	65	6.1	0.14
	BabakGair	21.362	1.51	1.01	2.09	−1.3	−0.50	−1.7	7.6	6.2	0.14
	EtfAG	—	54.0	4.88	−7375	26	17	—	—	32	0.83

[Babak+ 2010]

MLDC3: EMRis

Source (SNR_{true})	Group	SNR	$\frac{\delta M}{M}$ $\times 10^{-3}$	$\frac{\delta \mu}{\mu}$ $\times 10^{-3}$	$\frac{\delta \nu_0}{\nu_0}$ $\times 10^{-5}$	δe_0 $\times 10^{-3}$	$\delta \lvert S \rvert$ $\times 10^{-3}$	$\frac{\delta \lambda_{SL}}{\lambda_{SL}}$ $\times 10^{-3}$	δspin (deg)	δsky (deg)	$\frac{\delta D}{D}$
EMRI-1	MTAPCIOA	21.794	5.05	3.29	1.61	−5.1	−1.4	−19	23	2.0	0.07
(21.673)	MTAPCIOA	21.804	−0.06	−0.01	−0.08	−0.05	0.02	0.54	3.5	1.0	0.13
EMRI-2	MTAPCIOA	32.387	−3.64	−2.61	−3.09	3.8	0.87	12	11	3.7	3×10^{-3}
(32.935)	BabakGair	22.790	33.1	−19.7	10.1	−33	−7.3	25	47	3.5	−0.25
	BabakGair	22.850	32.7	−20.0	9.94	−32	−7.2	25	58	3.5	−0.24
	BabakGair	22.801	33.5	−19.5	10.5	−33	−7.4	240	40	3.5	−0.25
EMRI-3	MTAPCIOA	19.598	1.62	0.38	−0.10	−0.35	−0.94	−3.0	5.0	3.0	−0.04
(19.507)	BabakGair	21.392	1.77	1.01	1.95	−1.2	−0.68	−2.3	116	4.5	0.13
	BabakGair	21.364	2.26	1.88	2.71	−2.0	−0.69	−2.5	65	6.1	0.14
	BabakGair	21.362	1.51	1.01	2.09	−1.3	−0.50	−1.7	7.6	6.2	0.14
	EtfAG	—	54.0	4.88	−7375	26	17	—	—	32	0.83

[Babak+ 2010]

MLDC3: EMRis

Source ($\mathrm{SNR_{true}}$)	Group	SNR	$\frac{\delta M}{M}$ $\times 10^{-3}$	$\frac{\delta \mu}{\mu}$ $\times 10^{-3}$	$\frac{\delta \nu_0}{\nu_0}$ $\times 10^{-5}$	δe_0 $\times 10^{-3}$	$\delta\lvert S\rvert$ $\times 10^{-3}$	$\frac{\delta \lambda_{SL}}{\lambda_{SL}}$ $\times 10^{-3}$	δspin (deg)	δsky (deg)	$\frac{\delta D}{D}$
EMRI-1	MTAPCIOA	21.794	5.05	3.29	1.61	-5.1	-1.4	-19	23	2.0	0.07
(21.673)	MTAPCIOA	21.804	-0.06	-0.01	-0.08	-0.05	0.02	0.54	3.5	1.0	0.13
EMRI-2	MTAPCIOA	32.387	-3.64	-2.61	-3.09	3.8	0.87	12	11	3.7	3×10^{-3}
(32.935)	BabakGair	22.790	33.1	-19.7	10.1	-33	-7.3	25	47	3.5	-0.25
	BabakGair	22.850	32.7	-20.0	9.94	-32	-7.2	25	58	3.5	-0.24
	BabakGair	22.801	33.5	-19.5	10.5	-33	-7.4	240	40	3.5	-0.25
EMRI-3	MTAPCIOA	19.598	1.62	0.38	-0.10	-0.35	-0.94	-3.0	5.0	3.0	-0.04
(19.507)	BabakGair	21.392	1.77	1.01	1.95	-1.2	-0.68	-2.3	116	4.5	0.13
	BabakGair	21.364	2.26	1.88	2.71	-2.0	-0.69	-2.5	65	6.1	0.14
	BabakGair	21.362	1.51	1.01	2.09	-1.3	-0.50	-1.7	7.6	6.2	0.14
	EtfAG	—	54.0	4.88	-7375	26	17	—	—	32	0.83

[Babak+ 2010]

Model independent solution

- We still do not have a reliable complete model for generic orbits in Kerr
- Can we detect EMRIs? $\rightarrow$ **YES**

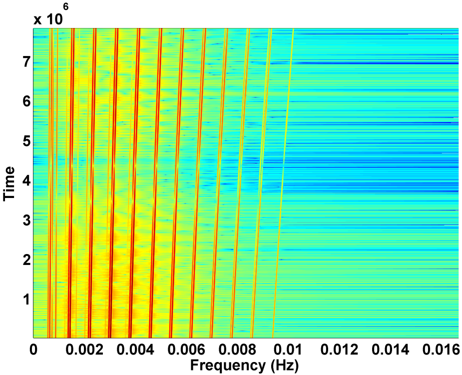

Harmonics of slowly varying orbital frequencies f_ϕ, f_r, f_θ.

Model independent solution

- We still do not have a reliable complete model for generic orbits in Kerr
- Can we detect EMRIs? $\rightarrow$ **YES**

$$h(t) = \sum_{l,m,n} h_{lmn}(t) = \mathrm{Re}\left(\sum_{l,m,n} A_{lmn}(t) e^{i(l\phi_r + m\phi_\theta + n\phi_\varphi)}\right),$$

where

$$\begin{aligned}
\phi_r(t) &= \phi_r(t_0) + \omega_r(t_0)(t-t_0) + \frac{1}{2}\dot{\omega}_r(t-t_0)^2 + \ldots \\
\phi_\theta(t) &= \phi_\theta(t_0) + \omega_\theta(t_0)(t-t_0) + \frac{1}{2}\dot{\omega}_\theta(t-t_0)^2 + \ldots \\
\phi_\varphi(t) &= \phi_\varphi(t_0) + \omega_\varphi(t_0)(t-t_0) + \frac{1}{2}\dot{\omega}_\varphi(t-t_0)^2 + \ldots \\
A_{lmn}(t) &= A_{lmn}(t_0) + \dot{A}_{lmn}(t_0)(t-t_0) + \ldots .
\end{aligned}$$

Model independent solution

- We still do not have a reliable complete model for generic orbits in Kerr
- Can we detect EMRIs? $\rightarrow$ **YES**

$$h(t) = \sum_{l,m,n} h_{lmn}(t) = \mathrm{Re}\left(\sum_{l,m,n} A_{lmn}(t) e^{i(l\phi_r + m\phi_\theta + n\phi_\varphi)}\right),$$

where

$$\begin{aligned}
\phi_r(t) &= \phi_r(t_0) + \omega_r(t_0)(t - t_0) + \frac{1}{2}\dot{\omega}_r(t - t_0)^2 + \dots \\
\phi_\theta(t) &= \phi_\theta(t_0) + \omega_\theta(t_0)(t - t_0) + \frac{1}{2}\dot{\omega}_\theta(t - t_0)^2 + \dots \\
\phi_\varphi(t) &= \phi_\varphi(t_0) + \omega_\varphi(t_0)(t - t_0) + \frac{1}{2}\dot{\omega}_\varphi(t - t_0)^2 + \dots \\
A_{lmn}(t) &= A_{lmn}(t_0) + \dot{A}_{lmn}(t_0)(t - t_0) + \dots .
\end{aligned}$$

Model independent solution

- Using introduced phenomenological waveform we could recover harmonics of the signal.
- Need a model (evolution of each harmonic $\rightarrow$ amplitude and frequency) to recover parameters of EMRI

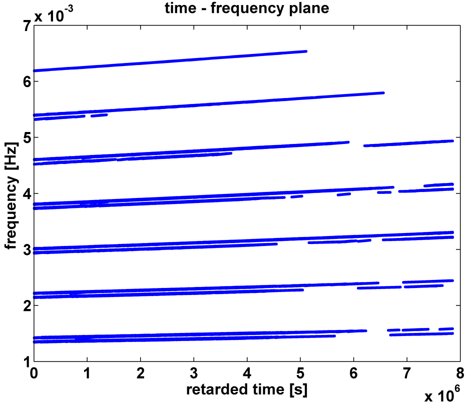

[Wang Yan+ 2012]

Parameter estimation

- Rich structure allows ultra-precise parameter estimation, including measuring the multipole moments of a central massive object (holiodesy)

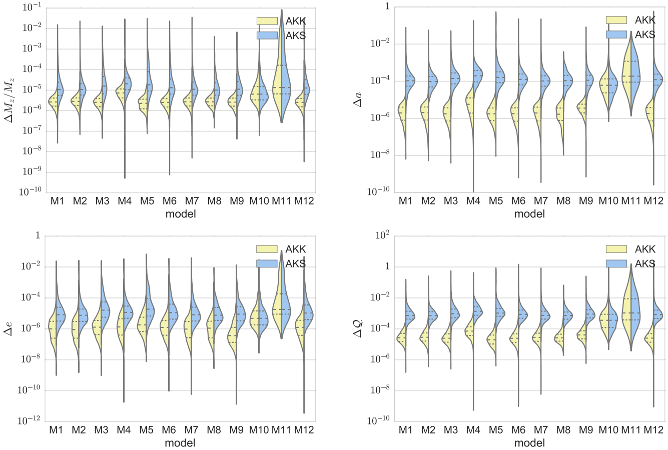

[Babak+ (2017)]

EMRIs: cosmology

- A single EMRI event with an electromagnetic counterpart (and hence a redshift measurement) will give the Hubble constant to an accuracy of $\sim 3\%$. N events give an accuracy of $\sim 3/\sqrt{N}\%$.
- Even without a counterpart, can estimate Hubble constant statistically [McLeod & Hogan 2008].
  1. Let every galaxy in the LISA error box "vote" on the Hubble constant
  2. If ~ 20 EMRI events are detected at $z < 0.5$, will determine the Hubble constant to $\sim 1\%$.
  3. Determining redshifts of all galaxies in the error box at $z < 0.5$ is already possible technologically.

EMRIs: cosmology

- A single EMRI event with an electromagnetic counterpart (and hence a redshift measurement) will give the Hubble constant to an accuracy of $\sim 3\%$. N events give an accuracy of $\sim 3/\sqrt{N}\%$.
- Even without a counterpart, can estimate Hubble constant statistically [McLeod & Hogan 2008].
  1. Let every galaxy in the LISA error box "vote" on the Hubble constant
  2. If ~ 20 EMRI events are detected at $z < 0.5$, will determine the Hubble constant to $\sim 1\%$.
  3. Determining redshifts of all galaxies in the error box at $z < 0.5$ is already possible technologically.

EMRIs: cosmology

- A single EMRI event with an electromagnetic counterpart (and hence a redshift measurement) will give the Hubble constant to an accuracy of $\sim 3\%$. N events give an accuracy of $\sim 3/\sqrt{N}\%$.
- Even without a counterpart, can estimate Hubble constant statistically [McLeod & Hogan 2008].
  1. Let every galaxy in the LISA error box "vote" on the Hubble constant
  2. If ~ 20 EMRI events are detected at $z < 0.5$, will determine the Hubble constant to $\sim 1\%$.
  3. Determining redshifts of all galaxies in the error box at $z < 0.5$ is already possible technologically.

EMRIs: cosmology

- A single EMRI event with an electromagnetic counterpart (and hence a redshift measurement) will give the Hubble constant to an accuracy of $\sim 3\%$. N events give an accuracy of $\sim 3/\sqrt{N}\%$.
- Even without a counterpart, can estimate Hubble constant statistically [McLeod & Hogan 2008].
  1. Let every galaxy in the LISA error box "vote" on the Hubble constant
  2. If ~ 20 EMRI events are detected at $z < 0.5$, will determine the Hubble constant to $\sim 1\%$.
  3. Determining redshifts of all galaxies in the error box at $z < 0.5$ is already possible technologically.

EMRIs: cosmology

- A single EMRI event with an electromagnetic counterpart (and hence a redshift measurement) will give the Hubble constant to an accuracy of $\sim 3\%$. N events give an accuracy of $\sim 3/\sqrt{N}\%$.
- Even without a counterpart, can estimate Hubble constant statistically [McLeod & Hogan 2008].
  1. Let every galaxy in the LISA error box "vote" on the Hubble constant
  2. If ~ 20 EMRI events are detected at $z < 0.5$, will determine the Hubble constant to $\sim 1\%$.
  3. Determining redshifts of all galaxies in the error box at $z < 0.5$ is already possible technologically.

EMRIs: fundamental science

- Black Hole Hypothesis - massive compact objects observed in the center of galaxies are spinning black holes described by the Kerr metric of Relativity. Use EMRIs to verify this.
- Extreme mass ratio ensures that the inspiralling object acts like a test particle. Use emitted gravitational waves to map out the spacetime structure.
- Deviations:
  1. Astrophysical perturbations, i.e. not a clean two-body problem
  2. Exotic central object, consistent with Relativity, e.g., a Boson Star.
  3. One of the assumptions of the uniqueness theorem is violated, e.g., axisymmetry, presence of a horizon, no closed-timelike-curves.
  4. Breakdown of the theory of Relativity in the strong field

EMRIs: fundamental science

- Black Hole Hypothesis - massive compact objects observed in the center of galaxies are spinning black holes described by the Kerr metric of Relativity. Use EMRIs to verify this.
- Extreme mass ratio ensures that the inspiralling object acts like a test particle. Use emitted gravitational waves to map out the spacetime structure.
- Deviations:
  1. Astrophysical perturbations, i.e. not a clean two-body problem
  2. Exotic central object, consistent with Relativity, e.g., a Boson Star.
  3. One of the assumptions of the uniqueness theorem is violated, e.g., axisymmetry, presence of a horizon, no closed-timelike-curves.
  4. Breakdown of the theory of Relativity in the strong field

EMRIs: fundamental science

- Black Hole Hypothesis - massive compact objects observed in the center of galaxies are spinning black holes described by the Kerr metric of Relativity. Use EMRIs to verify this.
- Extreme mass ratio ensures that the inspiralling object acts like a test particle. Use emitted gravitational waves to map out the spacetime structure.
- Deviations:
  1. Astrophysical perturbations, i.e. not a clean two-body problem
  2. Exotic central object, consistent with Relativity, e.g., a Boson Star.
  3. One of the assumptions of the uniqueness theorem is violated, e.g., axisymmetry, presence of a horizon, no closed-timelike-curves.
  4. Breakdown of the theory of Relativity in the strong field

EMRIs: fundamental science

- Black Hole Hypothesis - massive compact objects observed in the center of galaxies are spinning black holes described by the Kerr metric of Relativity. Use EMRIs to verify this.
- Extreme mass ratio ensures that the inspiralling object acts like a test particle. Use emitted gravitational waves to map out the spacetime structure.
- Deviations:
  1. Astrophysical perturbations, i.e. not a clean two-body problem
  2. Exotic central object, consistent with Relativity, e.g., a Boson Star.
  3. One of the assumptions of the uniqueness theorem is violated, e.g., axisymmetry, presence of a horizon, no closed-timelike-curves.
  4. Breakdown of the theory of Relativity in the strong field

EMRIs: fundamental science

- Black Hole Hypothesis - massive compact objects observed in the center of galaxies are spinning black holes described by the Kerr metric of Relativity. Use EMRIs to verify this.
- Extreme mass ratio ensures that the inspiralling object acts like a test particle. Use emitted gravitational waves to map out the spacetime structure.
- Deviations:
  1. Astrophysical perturbations, i.e. not a clean two-body problem
  2. Exotic central object, consistent with Relativity, e.g., a Boson Star.
  3. One of the assumptions of the uniqueness theorem is violated, e.g., axisymmetry, presence of a horizon, no closed-timelike-curves.
  4. Breakdown of the theory of Relativity in the strong field

EMRIs: fundamental science

- Black Hole Hypothesis - massive compact objects observed in the center of galaxies are spinning black holes described by the Kerr metric of Relativity. Use EMRIs to verify this.
- Extreme mass ratio ensures that the inspiralling object acts like a test particle. Use emitted gravitational waves to map out the spacetime structure.
- Deviations:
  1. Astrophysical perturbations, i.e. not a clean two-body problem
  2. Exotic central object, consistent with Relativity, e.g., a Boson Star.
  3. One of the assumptions of the uniqueness theorem is violated, e.g., axisymmetry, presence of a horizon, no closed-timelike-curves.
  4. Breakdown of the theory of Relativity in the strong field

Testing "No-hair" theorem

- Can characterize a vacuum, axisymmetric spacetime in GR by its multipole moments. For a Kerr black hole, these satisfy the "no-hair" theorem:

$$M_k + iS_k = M(ia)^k$$

- Multipole moments are encoded in gravitational wave observables - precession frequencies & number of cycles [Ryan 1995]

Testing "No-hair" theorem

- Can characterize a vacuum, axisymmetric spacetime in GR by its multipole moments. For a Kerr black hole, these satisfy the "no-hair" theorem:

$$M_k + iS_k = M(ia)^k$$

- Multipole moments are encoded in gravitational wave observables - precession frequencies & number of cycles [Ryan 1995]

- Collins & Hughes (2004) - considered a perturbed Schwarzschild black hole. Compared perihelion precession rates for eccentric orbits.
- Glampedakis & Babak (2006) - constructed a “quasi-Kerr” spacetime that was a perturbed Kerr black hole. Explored dephasing of geodesic orbits.
- Barack & Cutler (2007) - considered kludged post-Newtonian inspirals in a spacetime with an excess quadrupole moment. Fisher matrix analysis indicated the quadrupole moment could be measured to $\sim 0.1\%$.
- Gair, Li & Mandel (2008) - considered exact solutions of the GR field equations due to Manko and Novikov. Looked at precession rates for nearly circular and equatorial orbits.
- Sopuerta & Yunes (2009) - considered black holes in Chern-Simons gravity. Black holes in this theory differ from Kerr at fourth multipole moment. Modifies geodesic trajectories and hence waveform phasing.

- Collins & Hughes (2004) - considered a perturbed Schwarzschild black hole. Compared perihelion precession rates for eccentric orbits.
- Glampedakis & Babak (2006) - constructed a “quasi-Kerr” spacetime that was a perturbed Kerr black hole. Explored dephasing of geodesic orbits.
- Barack & Cutler (2007) - considered kludged post-Newtonian inspirals in a spacetime with an excess quadrupole moment. Fisher matrix analysis indicated the quadrupole moment could be measured to $\sim 0.1\%$.
- Gair, Li & Mandel (2008) - considered exact solutions of the GR field equations due to Manko and Novikov. Looked at precession rates for nearly circular and equatorial orbits.
- Sopuerta & Yunes (2009) - considered black holes in Chern-Simons gravity. Black holes in this theory differ from Kerr at fourth multipole moment. Modifies geodesic trajectories and hence waveform phasing.

- Collins & Hughes (2004) - considered a perturbed Schwarzschild black hole. Compared perihelion precession rates for eccentric orbits.
- Glampedakis & Babak (2006) - constructed a "quasi-Kerr" spacetime that was a perturbed Kerr black hole. Explored dephasing of geodesic orbits.
- Barack & Cutler (2007) - considered kludged post-Newtonian inspirals in a spacetime with an excess quadrupole moment. Fisher matrix analysis indicated the quadrupole moment could be measured to $\sim 0.1\%$.
- Gair, Li & Mandel (2008) - considered exact solutions of the GR field equations due to Manko and Novikov. Looked at precession rates for nearly circular and equatorial orbits.
- Sopuerta & Yunes (2009) - considered black holes in Chern-Simons gravity. Black holes in this theory differ from Kerr at fourth multipole moment. Modifies geodesic trajectories and hence waveform phasing.

- Collins & Hughes (2004) - considered a perturbed Schwarzschild black hole. Compared perihelion precession rates for eccentric orbits.
- Glampedakis & Babak (2006) - constructed a “quasi-Kerr” spacetime that was a perturbed Kerr black hole. Explored dephasing of geodesic orbits.
- Barack & Cutler (2007) - considered kludged post-Newtonian inspirals in a spacetime with an excess quadrupole moment. Fisher matrix analysis indicated the quadrupole moment could be measured to $\sim 0.1\%$.
- Gair, Li & Mandel (2008) - considered exact solutions of the GR field equations due to Manko and Novikov. Looked at precession rates for nearly circular and equatorial orbits.
- Sopuerta & Yunes (2009) - considered black holes in Chern-Simons gravity. Black holes in this theory differ from Kerr at fourth multipole moment. Modifies geodesic trajectories and hence waveform phasing.

- Collins & Hughes (2004) - considered a perturbed Schwarzschild black hole. Compared perihelion precession rates for eccentric orbits.
- Glampedakis & Babak (2006) - constructed a “quasi-Kerr” spacetime that was a perturbed Kerr black hole. Explored dephasing of geodesic orbits.
- Barack & Cutler (2007) - considered kludged post-Newtonian inspirals in a spacetime with an excess quadrupole moment. Fisher matrix analysis indicated the quadrupole moment could be measured to $\sim 0.1\%$.
- Gair, Li & Mandel (2008) - considered exact solutions of the GR field equations due to Manko and Novikov. Looked at precession rates for nearly circular and equatorial orbits.
- Sopuerta & Yunes (2009) - considered black holes in Chern-Simons gravity. Black holes in this theory differ from Kerr at fourth multipole moment. Modifies geodesic trajectories and hence waveform phasing.

- Li & Lovelace (2007) - studied tidal coupling interaction. Comparison of flux at infinity and inspiral rate reveals properties of central object.
- Barausse et al. (2007, 2008) studied influence of matter on inspirals; gravitational effect undetectable, but drag important.
- Berry & Gair (2011) - looked at inspirals in f(R) gravity; gravitational wave constraints better than Solar system observations but much weaker than lab bounds.
- Yunes et al. (2011) - signature of massive perturbers. Second SMBH within ~ 0.1 pc would leave detectable imprint.
- Canizares et.al. (2012) - inspirals in dynamic Chern-Simons gravity: extension of prev. work, includes inspiral and FIM: estimation of CS parameter to 5% accuracy or setting upper bound $\xi^{1/4} < 10^4$ km
- Gair & Yunes (2011) - kludge waveform in arbitrary modified gravity spacetime
- Barausse, Cardoso & Pani (2014) - Various environmental effects

- Li & Lovelace (2007) - studied tidal coupling interaction. Comparison of flux at infinity and inspiral rate reveals properties of central object.
- Barausse et al. (2007, 2008) studied influence of matter on inspirals; gravitational effect undetectable, but drag important.
- Berry & Gair (2011) - looked at inspirals in f(R) gravity; gravitational wave constraints better than Solar system observations but much weaker than lab bounds.
- Yunes et al. (2011) - signature of massive perturbers. Second SMBH within $\sim$ 0.1 pc would leave detectable imprint.
- Canizares et.al. (2012) - inspirals in dynamic Chern-Simons gravity: extension of prev. work, includes inspiral and FIM: estimation of CS parameter to 5% accuracy or setting upper bound $\xi^{1/4} < 10^4$ km
- Gair & Yunes (2011) - kludge waveform in arbitrary modified gravity spacetime
- Barausse, Cardoso & Pani (2014) - Various environmental effects

- Li & Lovelace (2007) - studied tidal coupling interaction. Comparison of flux at infinity and inspiral rate reveals properties of central object.
- Barausse et al. (2007, 2008) studied influence of matter on inspirals; gravitational effect undetectable, but drag important.
- Berry & Gair (2011) - looked at inspirals in f(R) gravity; gravitational wave constraints better than Solar system observations but much weaker than lab bounds.
- Yunes et al. (2011) - signature of massive perturbers. Second SMBH within ~ 0.1 pc would leave detectable imprint.
- Canizares et.al. (2012) - inspirals in dynamic Chern-Simons gravity: extension of prev. work, includes inspiral and FIM: estimation of CS parameter to 5% accuracy or setting upper bound $\xi^{1/4} < 10^4$ km
- Gair & Yunes (2011) - kludge waveform in arbitrary modified gravity spacetime
- Barausse, Cardoso & Pani (2014) - Various environmental effects

- Li & Lovelace (2007) - studied tidal coupling interaction. Comparison of flux at infinity and inspiral rate reveals properties of central object.
- Barausse et al. (2007, 2008) studied influence of matter on inspirals; gravitational effect undetectable, but drag important.
- Berry & Gair (2011) - looked at inspirals in f(R) gravity; gravitational wave constraints better than Solar system observations but much weaker than lab bounds.
- Yunes et al. (2011) - signature of massive perturbers. Second SMBH within $\sim$ 0.1 pc would leave detectable imprint.
- Canizares et.al. (2012) - inspirals in dynamic Chern-Simons gravity: extension of prev. work, includes inspiral and FIM: estimation of CS parameter to 5% accuracy or setting upper bound $\xi^{1/4} < 10^4$ km
- Gair & Yunes (2011) - kludge waveform in arbitrary modified gravity spacetime
- Barausse, Cardoso & Pani (2014) - Various environmental effects

- Li & Lovelace (2007) - studied tidal coupling interaction. Comparison of flux at infinity and inspiral rate reveals properties of central object.
- Barausse et al. (2007, 2008) studied influence of matter on inspirals; gravitational effect undetectable, but drag important.
- Berry & Gair (2011) - looked at inspirals in f(R) gravity; gravitational wave constraints better than Solar system observations but much weaker than lab bounds.
- Yunes et al. (2011) - signature of massive perturbers. Second SMBH within $\sim$ 0.1 pc would leave detectable imprint.
- Canizares et.al. (2012) - inspirals in dynamic Chern-Simons gravity: extension of prev. work, includes inspiral and FIM: estimation of CS parameter to 5% accuracy or setting upper bound $\xi^{1/4} < 10^4$ km
- Gair & Yunes (2011) - kludge waveform in arbitrary modified gravity spacetime
- Barausse, Cardoso & Pani (2014) - Various environmental effects

- Li & Lovelace (2007) - studied tidal coupling interaction. Comparison of flux at infinity and inspiral rate reveals properties of central object.
- Barausse et al. (2007, 2008) studied influence of matter on inspirals; gravitational effect undetectable, but drag important.
- Berry & Gair (2011) - looked at inspirals in f(R) gravity; gravitational wave constraints better than Solar system observations but much weaker than lab bounds.
- Yunes et al. (2011) - signature of massive perturbers. Second SMBH within $\sim$ 0.1 pc would leave detectable imprint.
- Canizares et.al. (2012) - inspirals in dynamic Chern-Simons gravity: extension of prev. work, includes inspiral and FIM: estimation of CS parameter to 5% accuracy or setting upper bound $\xi^{1/4} < 10^4$ km
- Gair & Yunes (2011) - kludge waveform in arbitrary modified gravity spacetime
- Barausse, Cardoso & Pani (2014) - Various environmental effects

- Li & Lovelace (2007) - studied tidal coupling interaction. Comparison of flux at infinity and inspiral rate reveals properties of central object.
- Barausse et al. (2007, 2008) studied influence of matter on inspirals; gravitational effect undetectable, but drag important.
- Berry & Gair (2011) - looked at inspirals in f(R) gravity; gravitational wave constraints better than Solar system observations but much weaker than lab bounds.
- Yunes et al. (2011) - signature of massive perturbers. Second SMBH within $\sim$ 0.1 pc would leave detectable imprint.
- Canizares et.al. (2012) - inspirals in dynamic Chern-Simons gravity: extension of prev. work, includes inspiral and FIM: estimation of CS parameter to 5% accuracy or setting upper bound $\xi^{1/4} < 10^4$ km
- Gair & Yunes (2011) - kludge waveform in arbitrary modified gravity spacetime
- Barausse, Cardoso & Pani (2014) - Various environmental effects

Summary

GW astronomy with EMRIs

- LISA is very strong now! LPF and 4 GWs with LIGO: full speed ahead with space-based project.
- We have considered formation of EMRIs and expected (observed) event rate ($\sim$ 100 EMRIs/year)
- The waveform modeling is required for accurate recovery parameters of EMRIs (underway)
- We know that we can detect single EMRI in Gaussian noise. Can we detect it in the source confused environment?
- If we pull those signals, we get vast amount of astro and fundamental physics information.